Heliyon 10 (2024) e32460

Contents lists available at ScienceDirect

Heliyon

journal homepage: www.cell.com/heliyon

Research article

Effects of myo-inositol on regulating glucose and lipid metabolism and alternative splicing events coexpressed with lncRNAs in the liver tissues of diabetic mice

Jin'e Li [a,b,1], Qiulan Huang [a,1], Qin Nie [d,1], Yunfei Luo [a], Haixia Zeng [a,b], Yuying Zhang [a,b], Xiaoju He [a,c], Jianping Liu [a,b,*]

[a] Department of Endocrinology and Metabolism of the Second Affiliated Hospital, Jiangxi Medical College, Nanchang University, Nanchang, 330006, Jiangxi, China
[b] Institute for the Study of Endocrinology and Metabolism in Jiangxi Province, Nanchang, 330006, Jiangxi, China
[c] Department of Obstetrics and Gynecology of the Second Affiliated Hospital, Jiangxi Medical College, Nanchang University, Nanchang, 330006, Jiangxi, China
[d] Zhongnan Hospital of Wuhan University, Wuhan, 430071, Hubei, China

ARTICLE INFO

Keywords:
Diabetes mellitus
Liver
Glucose and lipid metabolism
Myo-inositol
Alternative splicing
Long-noncoding RNA

ABSTRACT

Objective: Recent studies have shown that gene alternative splicing (AS) and long noncoding RNAs (lncRNAs) are involved in diabetes mellitus (DM) and its complications. Currently, myo-inositol (MI) is considered as effective for the treatment of insulin resistance and lipid metabolism disorders in diabetes patients. We hope to better explore the potential roles of gene AS and lncRNAs in liver glucose and lipid metabolism in diabetes, as well as the effects of myo-inositol treatment, through transcriptome analysis.

Methods: This study analysed glucose and lipid metabolism-related biochemical indicators and liver HE staining in four groups of mice: the control group (Ctrl group), the diabetes group (DM group), the myo-inositol treatment group (MI group), and the metformin treatment group (Met group). The changes in relevant gene-regulated alternative splicing events (RASEs) and lncRNAs were analysed by RNA sequencing of liver tissue, and coexpression analysis and functional enrichment analysis were used to predict the possible lncRNAs and RASEs involved in liver glucose and lipid metabolism.

Result: Metformin and myo-inositol alleviated insulin resistance, lipid metabolism disorders, and hepatic steatosis in diabetic mice. Transcriptome sequencing analysis revealed differential splicing events of genes related to lipid metabolism and differentially expressed lncRNAs (DElncRNAs). Six different lncRNAs and their potentially interacting splicing events were predicted.

Abbreviations: AS, Alternative splicing; LncRNA, long non-coding RNA; DM, Diabetes mellitus; MI, myo-inositol; Met, metformin; RASE, regulated alternative splicing event; DElncRNA, differentially expressed lncRNA; IR, insulin resistance; HOMA-IR, Homeostasis Model Assessment-Insulin Resistance; PPARγ, peroxisome proliferator-activated receptor γ; GLUT4, Glucose transporter type 4; FBG, Fasting blood glucose; RNA-Seq, RNA sequencing; FINS, fasting insulin; IPGTT, intraperitoneal glucose tolerance test; IPITT, intraperitoneal insulin tolerance test; STZ, streptozotocin; ES, exon skipping, cassette exon; A5SS, alternative 5'splice site; A3SS, alternative 3′ splice site; IR, intron retention; MXE, mutually exclusive exons; 5pMXE, 5pMXE, mutually exclusive 5′UTRs; 3pMXE, mutually exclusive 3′UTRs.

* Corresponding author. No.1, Minde Road, Nanchang, 330000, Jiangxi, China.
E-mail address: ndefy14105@ncu.edu.cn (J. Liu).

[1] These authors have contributed equally to this work.

https://doi.org/10.1016/j.heliyon.2024.e32460
Received 19 April 2023; Received in revised form 26 May 2024; Accepted 4 June 2024
Available online 5 June 2024

Conclusion: The present study revealed novel changes in RASEs and lncRNAs in the livers of diabetic mice following treatment with myo-inositol, which may shed light on the potential mechanisms by which myo-inositol delays and treats the progression of hepatic glucose and lipid metabolism in diabetes.

1. Introduction

At present, the prevalence of diabetes mellitus (DM) is rapidly increasing worldwide. According to the latest data from the International Diabetes Federation, there will be 537 million adults with diabetes worldwide, approximately 90 % of whom will have type 2 diabetes mellitus (T2DM) by 2021 [1]. T2DM is mainly characterized by relative insulin deficiency caused by abnormal pancreatic β-cell function and the insulin resistance (IR) of target organs such as the liver and skeletal muscle. As the main organ related to sugar and lipid metabolism, the liver's sensitivity to insulin decreases when it undergoes fatty degeneration, and the inhibitory effect of insulin on glucose production decreases [2,3]. The use of insulin-sensitizing agents is significant for preventing and delaying the progression of T2DM.

Inositol is an insulin sensitizer with the potential to modulate insulin sensitivity in animal models and insulin-resistant patients [4,5]. In a mouse model of diabetes induced by a high-fat diet and streptozotocin (STZ), inositol treatment reduced plasma insulin and HOMA-IR levels while promoting the expression of PPARγ and GLUT4 in adipose tissue [6]. In a study involving patients with T2DM who had poor glycaemic control and were receiving hypoglycaemic medication, as well as a combination of oral myo-inositol and d-chiro-inositol as an additional supplement for three months, it was shown that in addition to a significant decrease in fasting blood glucose (FBG) and haemoglobin A1c levels in comparison to baseline, there was also a reduction in the accumulation of triglycerides and a decrease in the expression of genes associated with fat synthesis in the livers of rats fed a high-fructose diet [7]. Myo-inositol (MI) is the most abundant isomer of inositol in living cells and food, making it one of the best candidates for nutritional strategies [8].

Alternative splicing (AS) events and epigenetic analysis using RNA sequencing (RNA-Seq) have become increasingly important tools in the study of diabetes and liver metabolism [9,10]. AS plays a critical role in regulating transcription processes in almost every aspect of eukaryotic biology, allowing cells to generate multiple protein isoforms from a single gene [11]. Some studies suggest that AS is involved in diabetes and diabetic vasculopathy [12,13]. An in-depth investigation of AS complexity in the transcriptome by high-throughput sequencing has also shed light on the critical role of AS in cellular processes [14,15]. Numerous studies have demonstrated that AS is influenced by epigenetic factors, such as long noncoding RNAs [16,17]. Nonetheless, investigations of AS events and analysis of coexpression with lncRNAs in diabetic mouse models using RNA-Seq data are currently scarce. Consequently, it remains unclear whether MI has any impact on diabetic lipid metabolism, liver gene variable splicing, or lncRNA regulation.

To summarize, we constructed mouse models of diabetes to explore the impact of MI on AS and lncRNAs, as well as the potential lncRNA/regulated alternative splicing event (RASE) mechanism of liver genes in diabetic glycolipid metabolism and hepatic steatosis.

2. Material and methods

2.1. Establishment of animal model

All animal experimentation was approved by Experimental Animal Welfare Ethics Committee of Nanchang University (Approval No. NCULAE-20221031042) and was in compliance with the ARRIVE guidelines. Male C57BL/6J mice, 4-week-old and weighing 20 ±2g, were raised in a standard environment. After one week of adaptation feeding, only those in good health were randomly assigned to one of the two groups: the standard chow diet group (Ctrl group) and the high-fat diet group containing 60 % kcal from fat. Six weeks later, the mice in the high-fat diet group were treated with STZ at a dose of 60 mg/kg by intraperitoneal injection for three consecutive times, while the Ctrl group was given saline. After 3 days of injection, the blood glucose levels of the mice were measured. Once the random blood glucose level was higher than 16.7 mmol/L for three consecutive days, the diabetes model was considered established successfully. These mice were then randomly divided into three groups: diabetes group (DM group), myo-inositol group (MI group), and metformin group (Met group). The MI and Met groups received daily intragastric administration of 800 mg/kg myo-inositol and 300 mg/kg metformin, respectively [18]. Both the Ctrl and DM groups received daily intragastric administration of ddH2O. The intragastric administration lasted for 4 weeks.

2.2. Biochemical criterion detection

2.2.1. Intraperitoneal glucose and insulin tolerance test (IPGTT and IPITT)

IPGTTs were performed by intraperitoneal (i.p.) injection of D-glucose (1.5 g/kg) after 12 h of fasting. IPITTs were performed by i.p. injection of 0.8 unit/kg insulin after 6 h of fasting. Blood glucose levels were recorded before and at15, 30, 60, 90, and 120 min after injection. IPGTTs and IPITTs were performed at third and fourth week after intragastric administration, respectively. The area under the curve (AUC) of the IPGTT or IPITT blood glucose was calculated using a formula.

2.2.2. Detection of serum biochemical markers

Whole blood was collected by eye orbit, and the supernatant was extracted from the blood samples and stored in a −80 °C

refrigerator. The levels of FBG, total cholesterol (TC), low-density lipoprotein cholesterol (LDL-C), triglycerides (TG), and high-density lipoprotein cholesterol (HDL-C) were measured by an automatic biochemical analysis instrument (BIOBASE, China). Serum alanine aminotransferase (ALT) and aspartate aminotransferase (AST) activities were measured using commercial kits (Solarbio, Beijing, China).

2.3. RNA sequencing and Bioinformation analysis

2.3.1. RNA sequencing

(1) RNA extraction and sequencing

Total RNAs were extracted from mouse liver tissues using TRIzol Reagent (Invitrogen, cat. NO 15596026). DNA digestion was carried out after RNA extraction by DNaseI. RNA quality was determined by examining A260/A280 with NanodropTM OneCspectrophotometer (Thermo Fisher Scientific Inc). RNA Integrity was confirmed by 1.5 % agarose gel electrophoresis. Qualified RNAs were finally quantified by Qubit3.0 with QubitTM RNA Broad Range Assay kit(Life Technologies,Q10210). 2 μg total RNAs were used for stranded RNA sequencing library preparation using KCTM Stranded mRNA Library Prep Kit for Illumina (Catalog NO. DR08402, Wuhan Seqhealth Co., Ltd. China) following the manufacturer's instruction. PCR products corresponding to 200–500 bps were enriched, quantified and finally sequenced on MGISEQ-T7(MGI) with PE150 model.

2.3.2. Bioinformation analysis

(1) Alternative splicing analysis

Alternative splicing events mainly include ten categories: exon skipping (ES), cassette exon, alternative 5′ splice site (A5SS), and alternative 3'splice site (A3SS), intron retention (IR), mutually exclusive exons (MXE), mutually exclusive 5′UTRs (5pMXE), mutually exclusive 3′UTRs(3pMXE), alternative 5′ splice site & exon skipping (A5SS&ES), and alternative 3′ splice site & exon skipping (A3SS&ES).

The alternative splicing events (ASEs) and RASEs between the samples were defined and quantified using the previously described ABLas pipeline [12]. After detecting the ASEs in each RNA-seq sample, a paired *t*-test was performed to compare the changed ratio of alternatively spliced reads and constitutively spliced reads between the two comparison groups. A P value < 0.05 was set as the threshold for RASE detection, which enabled us to compare changes in the alternative splicing levels of the same splicing type of each gene.

(2) LncRNA prediction

In order to predict credible lncRNA, we used four software to predict lncRNA: CPC2, LGC, CNCI and CPAT.We counted the non-coding transcripts identified by the above four analysis software. After the above steps, we successively removed the transcripts that overlap with the known coding genes, are less than 200bp in length, have potential coding ability, and are less than 1000bp away from the nearest gene from the assembly results, obtained the prediction results of new lncRNA, and used the intersection of the four software for subsequent analysis and processing.

(3) Functional enrichment analysis

To sort out functional categories of DEGs, Gene Ontology (GO) terms and KEGG pathways were identified using KOBAS 2.0 server. Hyper geometric test and Benjamini-Hochberg FDR controlling procedure were used to define the enrichment of each term.

2.4. Real-time quantitative PCR

The experiment commenced with the extraction of total RNA using the Trizol method. Subsequently, the RNA was converted into complementary DNA (cDNA) utilizing both the efficient FastQuant RT Kit (Tiangen, KR106) and the precise QuantScript RT Kit (Tiangen, KR103). Gene expression levels were then quantified through quantitative PCR, employing the SYBR Green Master Mix (Yeasen, 11184ES) following the manufacturer's recommended protocol. The 2-ΔΔCT method was utilized to calculate relative RNA expression levels, with GAPDH serving as the internal control for normalization. Detailed information regarding primer usage can be found in Supplementary File: Table SI.

Furthermore, an RT-qPCR assay was employed to analyze ASEs. A boundary-spanning primer for the sequence encompassing the junction of constitutive exon and alternative exon was used in conjunction with an opposing primer in a constitutive exon to detect alternative isoforms. The boundary-spanning primer of alternative exon was designed according to either "model exon" or "altered exon" to detect model splicing or altered splicing respectively. Primers for quantitative PCR analysis are presented in Table SI.

2.5. Cell culture

Human liver cancer cell line (HepG2, catalogue number: HB-8065) was purchased from the Cell bank of the Chinese Academy of Science (Shanghai, China). HepG2 cells were cultured in DMEM medium (Gibco™, Thermo Fisher, 11995040) containing 10 % fetal bovine serum (FBS; Gibco™, Thermo Fisher, 1600-044) at 37 °C with 5 % CO_2. Cells were divided into Control group, model group and model + MI group. Control group was cultured in low-glucose DMEM, while the model group was stimulated with high-glucose DMEM supplemented with 0.5 mM palmic acid for 24 h. MI with different concentrations (0.25, 0.5, 0.75, 1.0, and 2.0 mM) was added in medium for 24 h. Cell Counting Kit-8 (CCK8) (Wuhan Servicebio Technology) reagent was used to measure cell viability. The lowest effective concentration of MI was primarily set at 0.25, 0.5, 0.75, and 1.0 mM. D-glucose consumption was detected by Glucose detection kits (shanghai rongsheng Bioengineering Inst).

2.6. Statistical method

The experiment's data was statistically analysed using GraphPad Prism 8.3.0 software. One-way analysis of variance was employed to compare multiple groups, while t-tests were used for comparing two groups. The results were presented as mean ± standard error, with * indicating P values < 0.05, ** indicating P values < 0.01, and *** indicating P values < 0.001. A P value < 0.05 was considered indicative of a statistical difference.

3. Result

3.1. MI can improve glucose and lipid metabolism in HepG2 cells under conditions of high glucose and fat stimulation

In our in vitro cell experiments, we investigated the toxicity and minimum effective concentration of the MI drug. Based on the CCK-8 results, we observed a significant decrease in cell viability compared to that of the control group when the MI concentration was 2.0 mM (Fig. 1A), indicating a toxic effect. Additionally, the TG assay results showed a significant difference in lipid reduction effects at MI concentrations above 0.5 mM (Fig. 1B). Furthermore, the glucose consumption results also indicated that MI concentrations above 0.5 mM could enhance glucose metabolism (Fig. 1C).

3.2. The effect of MI on blood glucose and IR in diabetic mice

The fasting serum of the mice was collected after a four-week treatment period to determine the serum glucose and insulin levels. The results showed that the FBG levels in the DM group were significantly higher when compared with the control group. However, FBG levels decreased significantly in the MI and Met groups compared to those in the DM group, with no significant difference observed between the MI and Met groups (Fig. 2A). Compared with those in the control group, fasting insulin (FINS) levels in the DM group increased. Nevertheless, the FINS levels in the MI and Met groups showed a decreasing trend in comparison to those in the DM group, but the difference was not statistically significant (Fig. 2B). Additionally, after four weeks, the insulin resistance index (HOMA-IR), intraperitoneal glucose tolerance test (IPGTT) and intraperitoneal insulin tolerance test (IPITT) were performed (Fig. 2C–G). The results showed that the diabetic mice had a significantly impaired glucose tolerance and insulin resistance compared to normal mice. However, glucose tolerance and insulin resistance were significantly greater in the MI and Met groups than in the DM group, with no

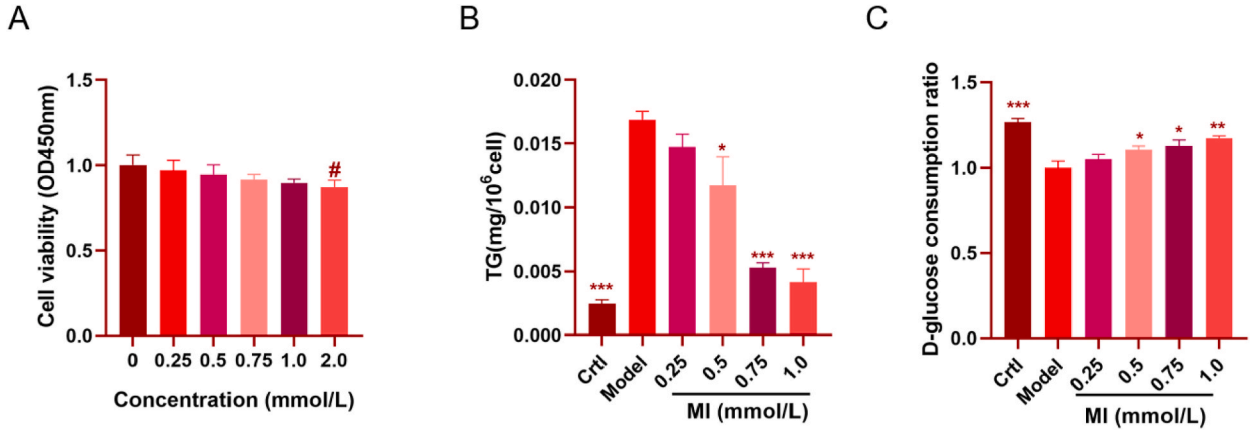

Fig. 1. The effect of MI on glucose consumption and lipid metabolism in HepG2 cells. (A) Effect of different concentrations of MI on the viability of HepG2 cells. (B) Effect of different concentrations of MI on the lipid reduction of HepG2 cells. (C) Effect of MI on glucose consumption in HepG2 cells. The # represents the comparison between different concentrations of MI groups and the blank group. ($P < 0.05$). The * indicates a comparison with the model group and other groups ($P < 0.05$).

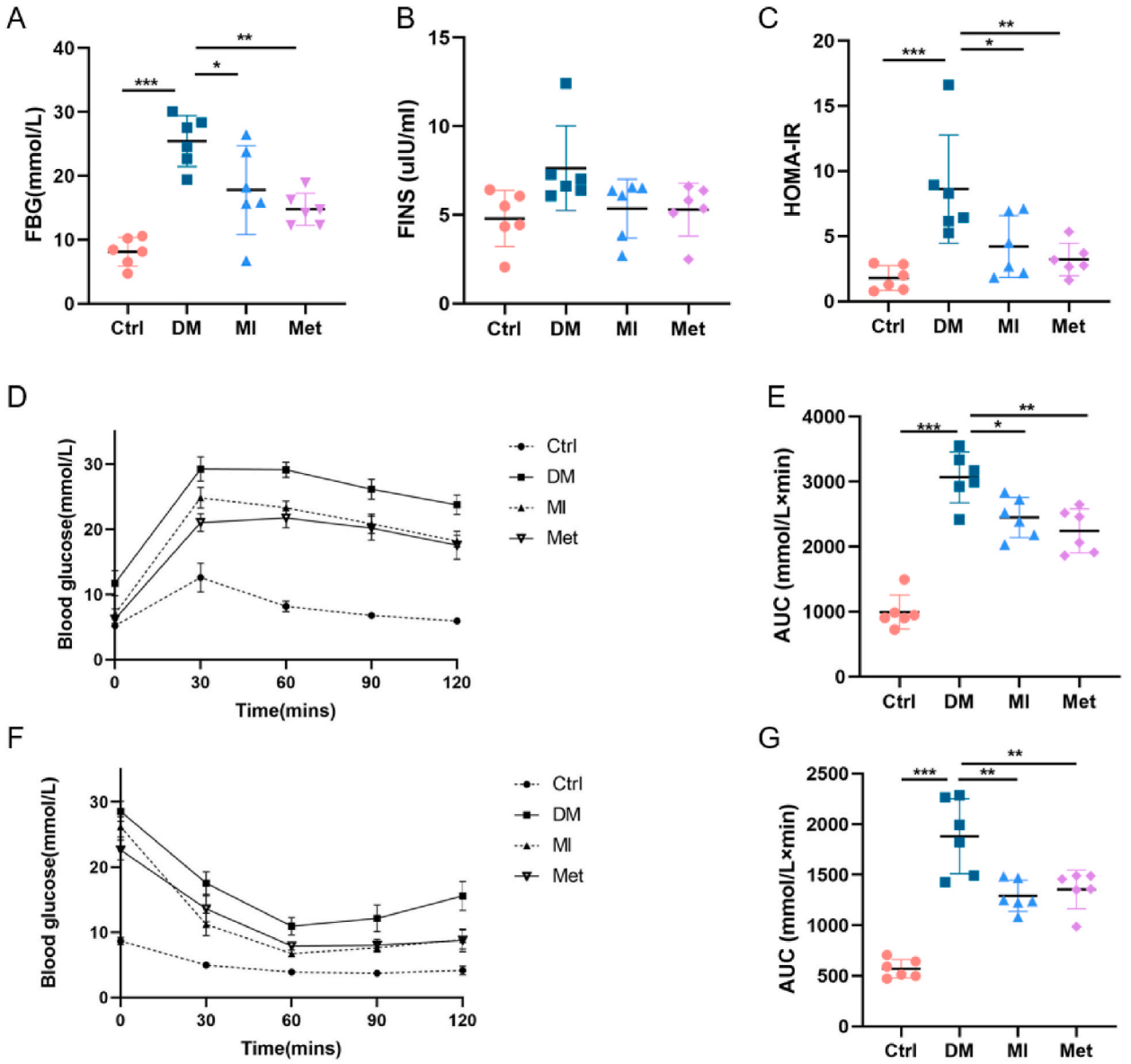

Fig. 2. The effect of MI on blood glucose and IR in diabetic mice. (A) Fasting blood glucose levels of mice in each group (n = 6). (B)Fasting serum insulin levels of mice in each group (n = 6). (C) HOMA-IR values of mice in each group (n = 6). (D) IPGTT of each group (n = 6). (E) Area under the curve of IPGTT. (F) IPITT of each group (n = 6). (G) Area under the curve of IPITT.

significant difference observed between the two groups.

3.3. Effect of MI on lipid metabolism in diabetic mice

After administering the treatment orally for four weeks, we examined lipid metabolism indices in the blood and liver of the mice. Our results showed that diabetic mice had significantly greater levels of TC and TG in both their serum and liver. However, treatment with MI or Met significantly reduced these levels, as shown in Fig. 3A–D. Furthermore, our study revealed that LDL-C levels were significantly decreased in both the MI and Met groups, but HDL-C levels remained unaffected (Fig. 3E–F). Notably, both the serum and liver TG levels in the MI group were significantly lower than those in the Met group (Fig. 3B and D). The detection of liver enzyme activity showed that MI could significantly improve the liver injury of diabetic mice with fatty liver, while Met could only significantly improve ALT (Fig. 3G–H).

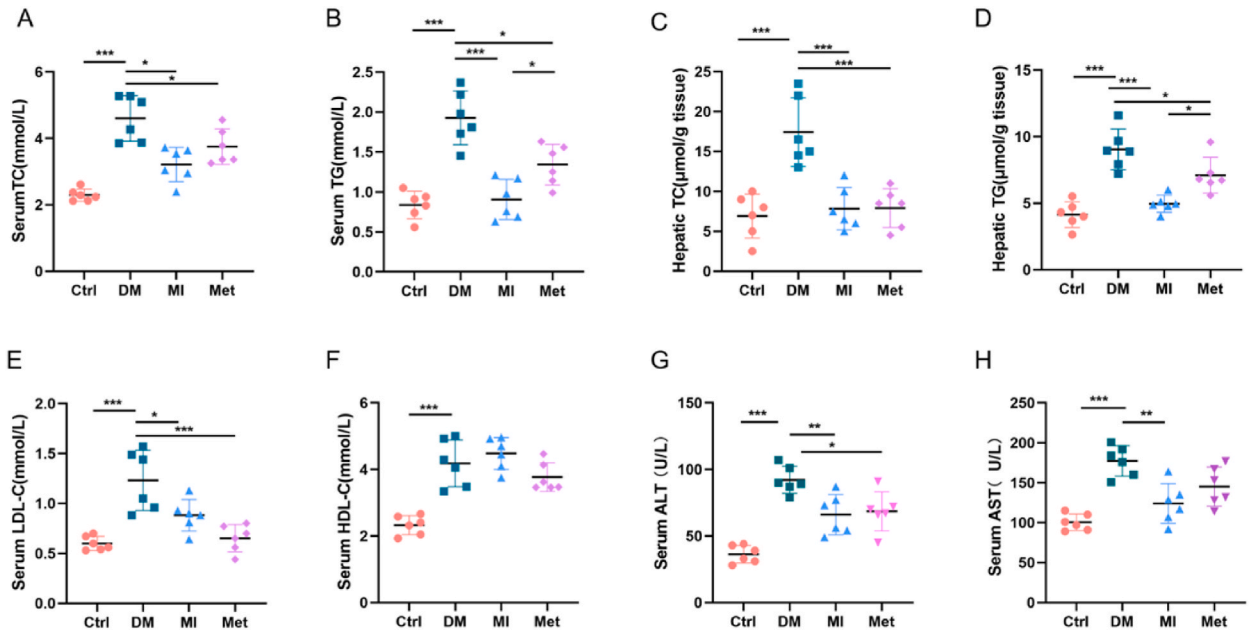

Fig. 3. Lipid content in serum and liver of mice in each group. A-D represent the serum levels and hepatic levels of total cholesterol (TC), triglycerides (TG); E-F represent the serum levels of low-density lipoprotein cholesterol (LDL-C), and high-density lipoprotein cholesterol (HDL-C). G-H represent the serum ALT and AST levels in mice.

3.4. Effect of MI on hepatic steatosis in diabetic mice

Hepatic pathology was examined by HE staining and Oil Red O staining in the mice. The livers of diabetic mice exhibited extensive hepatocyte steatosis, vacuolar lipid droplets of different sizes and infiltration of a few inflammatory cells. These findings suggested that hyperglycaemia worsens fatty liver disease. However, treatment with MI or Met significantly reduced the number of liver lipid droplets and inflammatory cells, as depicted in Fig. 4.

3.5. Different alternative splicing events occur throughout the liver tissue of diabetic mice

The plot of principal component analysis (PCA) demonstrated significant separations among the Ctrl, DM, and MI/Met groups (Fig. 5B). The RASE hierarchical clustering heatmap displayed variations in the expression of RASEs in each sample, with red indicating higher-level expression and green indicating lower-level expression (Fig. 5C).

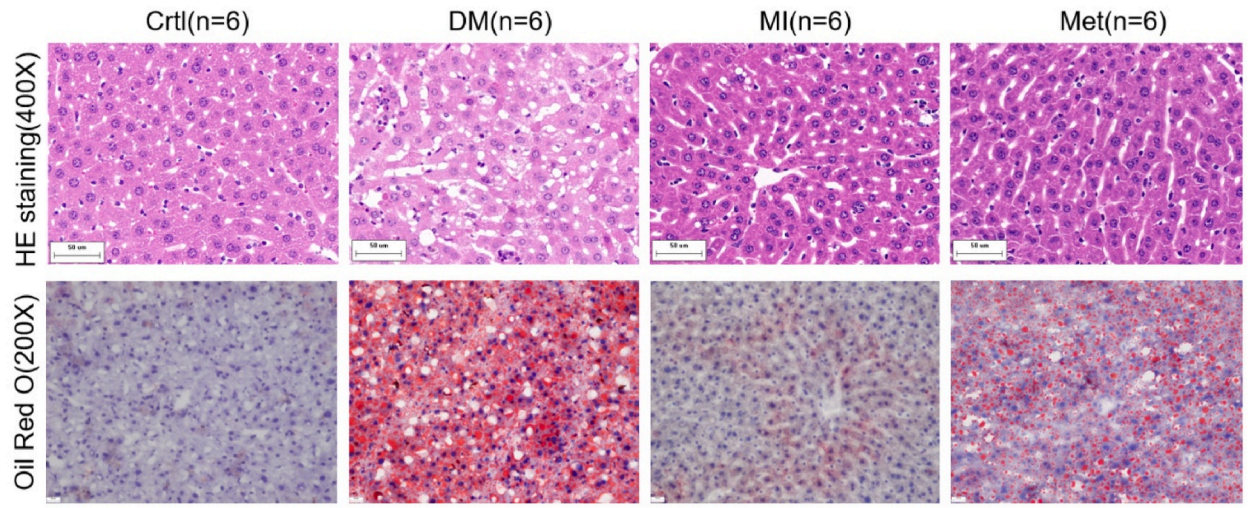

Fig. 4. Hepatic pathology by HE staining and Oil Red O staining (Scale bar = 50 μm) in mice of different groups (n = 6).

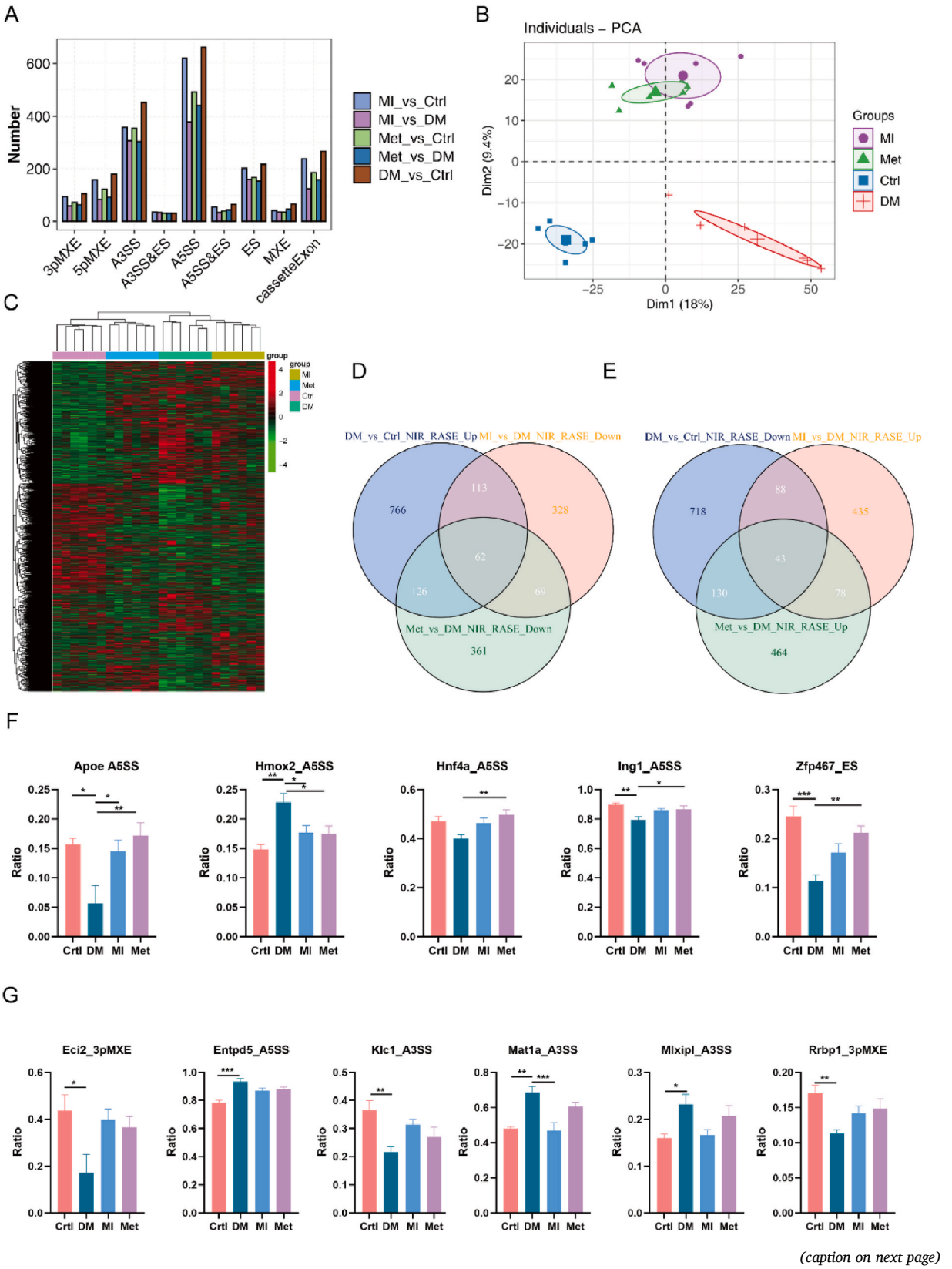

(caption on next page)

Fig. 5. The alternative splicing analysis of liver tissues of diabetes mice after metformin or myo-inositol treatment. (A) Bar plot showing the RASE numbers in the different types of AS events. (B) PCA of four groups of samples based on normalized NIR splicing ratio. (C) Hierarchical clustering heat map showing expression levels of all RASEs. (D–E) Venn diagram showing the overlapped RASEs between diabetes vs normal and myo-inositol/metformin vs diabetes. (F) The alternative splicing events regulated by diabetes after myo-inositol or metformin treatment. The boxplot shows alternative splicing events of *Apoe*, *Hnf4a, Ing1, Zfp467,* and *Hmox2*. (G) The alternative splicing events specific regulated by diabetes after myo-inositol treatment. The boxplot shows alternative splicing events of *Rrbp1, Eci2, Klc1, Mlxip1, Mat1a,* and *Entpd5*.

In the livers of diabetic mice, we observed a significant increase in 1067 RASEs, while 979 RASEs were decreased compared to those in normal mice. Among the 1067 upregulated RASEs, 62 RASEs were downregulated by both MI and Met, whereas 113 RASEs were downregulated specifically by MI therapy (Fig. 5D). Furthermore, 43 out of the 979 downregulated RASEs were elevated following treatment with both drugs, while 88 RASEs were specifically improved by MI therapy (Fig. 5E). Our analysis also revealed that A5SS and A3SS were the two most common types of RASEs (Fig. 5A and Table 1).

Based on the significant differences in the ratios between groups, we found that among the differentially spliced genes affected by both MI and Met, genes related to glucose and lipid metabolism or apoptosis included haem oxygenase 2 (*Homx2*), transcription factor finger protein 467 (*Zfp467*), hepatocyte nuclear factor 4a (*Hnf4a*), apoptosis-related gene inhibitor of growth 1 (*Ing1*), and lipid carrier protein apolipoprotein e (*Apoe*) (Fig. 5F), while RASGs specifically altered by MI included ectonucleoside triphosphate diphosphohydrolase 5 (*Entpd5*), methionine adenosyltransferase I alpha (*Mat1a*), transcription factor MLX interacting protein 1 (*Mlxip1*), insulin sensitivity-regulating kinesin light chain 1 (*Klc1*), lipid metabolism-related enoyl-CoA delta isomerase 2 (*Eci2*), and ribosome binding protein (*Rrbp1*) (Fig. 5G).

3.6. Differential expression of lncRNAs across liver tissue of diabetic mice

To determine the mechanism by which Met and MI affect glucolipid metabolism, we analysed lncRNA expression in the livers of C57BL/6J mice in different groups by RNA sequencing. The results of the PCA plot showed that there was a clear separation between the DM and Ctrl groups, with some overlap indicating an intersection of lncRNA differences between them (Fig. 6A). Our findings revealed that compared to those in the Ctrl group, 459 lncRNAs were upregulated and 59 lncRNAs were downregulated in the DM group (Fig. 6B). Among the 459 lncRNAs significantly increased in diabetic mice, 14 lncRNAs were downregulated by myo-inositol and metformin, and another 14 lncRNAs were downregulated by myo-inositol (Fig. 6C). Moreover, 3 lncRNAs exhibited increased expression after treatment with both drugs, and 2 lncRNAs increased specifically after MI treatment, among which 59 lncRNAs were downregulated in diabetic animal models (Fig. 6D).

The GO and KEGG functional enrichment analyses of the differentially expressed lncRNAs showed that they were enriched in the skeleton, cytoplasm and processes related to calcium ion transport, oxidation−reduction, and lipid metabolism (Figure SI). After screening key lncRNAs, it was found that the lncRNAs nuclear paraspeckle assembly transcript 1 (*Neat1*) and *Gm16551*, which regulate fat metabolism, and the lncRNA *Lockd*, which is related to glucose metabolism, may be important for reducing blood sugar and blood lipids and improving hepatic steatosis in MI. Among them, lncRNA *Gm16551* was shown to be altered by MI treatment but not by Met treatment (Fig. 6E–G). We further extracted RNA from mouse liver tissues for qPCR validation and found that compared to that in the control group, the expression of the lncRNA *Neat1* was significantly elevated in the DM group. In contrast, compared with those in the DM group, the expression of *Gm16551* in the MI-treated group was notably upregulated, consistent with our predictions (Fig. 6H).

3.7. Coexpression analysis and functional enrichment analysis of lncRNAs and RASEs in liver tissues of diabetic mice

LncRNAs play an important role in regulating alternative splicing. In this study, we performed a coexpression analysis of lncRNAs and RASEs to explore the possible mechanism of MI treatment in diabetes. The 17 lncRNAs (14 downregulated and 3 upregulated) whose expression was altered by both MI and Met treatment were coexpressed with the RASEs obtained in the above analysis. We selected pairs with Spearman correlation coefficients >0.8 and $P < 0.01$ between RASEs and DElncRNAs based on the RNA-seq data, and we observed that 17 lncRNAs were coexpressed with 205 RASEs (Fig. 7A). GO functional enrichment analysis was conducted for genes related to the 205 RASEs, which were primarily enriched in biological processes such as cellular response to insulin stimulus,

Table 1
Comparison between groups of changes in different alternative splicing types.

Sample	Type	3pMXE	5pMXE	A3SS	A3SS&ES	A5SS	A5SS&ES	ES	MXE	Cassette Exon	Total
DM_VS_Ctrl	Up	42	66	278	13	372	21	60	26	189	1067
DM_VS_Ctrl	Down	64	114	174	18	290	44	157	40	78	979
MI_VS_DM	Up	29	52	151	19	194	22	93	23	61	644
MI_VS_DM	Down	30	32	156	15	184	12	67	13	63	572
MI_VS_Ctrl	Up	42	61	235	20	354	24	82	22	173	1013
MI_VS_Ctrl	Down	52	97	122	16	267	31	120	20	65	790
Met_VS_DM	Up	33	44	162	17	221	30	97	30	81	715
Met_VS_DM	Down	30	48	142	14	220	14	56	17	77	618
Met_VS_Ctrl	Up	26	43	219	22	273	19	70	17	126	815
Met_VS_Ctrl	Down	46	80	135	9	219	21	97	18	60	685

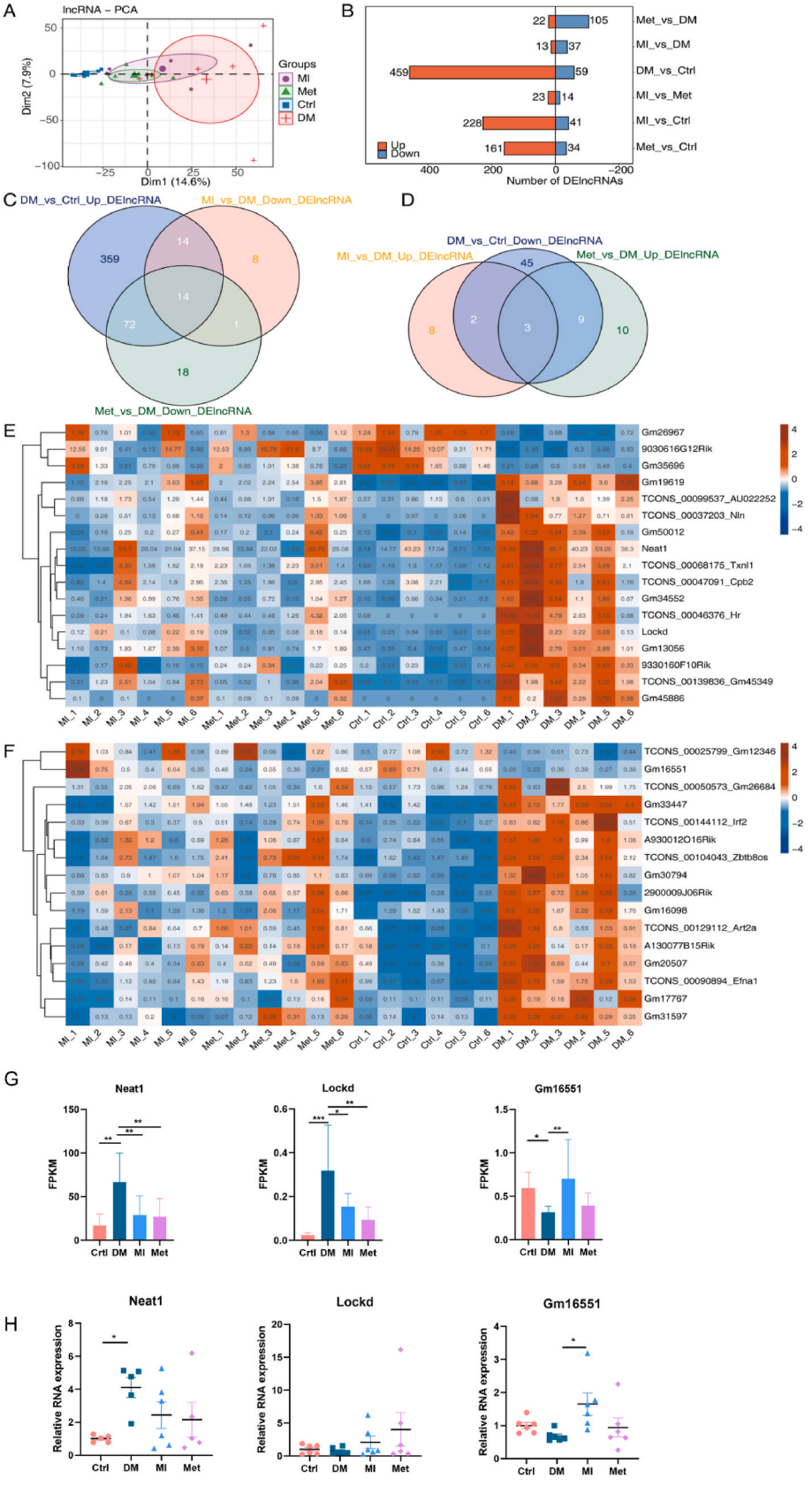

(caption on next page)

Fig. 6. Analysis of differential expression of lncRNAs in liver tissues of diabetes mice after myo-inositol treatment (A) PCA base on FPKM value of all detected lncRNA genes. The ellipse for each group is the confidence ellipse. (B) Bar plot showing all differentially expressed lncRNA genes with DESeq. P value < 0.01 and FC (fold change) ≥ 1.5 or ≤ 2/3. (C–D) Venn diagram showing the overlapped DElncRNAs between diabetes vs normal and myoinositol or metformin vs diabetes. (E–F) Hierarchical clustering heat map showing the expression pattern and statistical difference of DE-lncRNA genes. (G) The histogram shows the expression levels of lncRNA *Neat1, Lockd, and Gm16551* (n = 6). (H) The relative lncRNAs expression between diabetes vs normal and myoinositol or metformin vs diabetes.

oxidation−reduction process, translation, mRNA processing, lipid metabolism, phosphorylation, protein transport, protein hydrolysis, regulation of transcription by RNA polymerase I, and positive regulation of transcription by RNA polymerase II (Fig. 7B).

In addition, an overlap analysis was conducted between these 205 RASEs and 105 RASEs (62 downregulated and 43 upregulated) modified by MI and Met treatment. Two credible RASEs, glutathione S transferase a2 (*Gsta2*) A5SS&ES and 3 beta- and steroid delta-isomerase 3 (*Hsd3b3*) A3SS, were selected based on the significance of the difference in the ratio between the groups. Coexpression analysis revealed that *Gsta2* A5SS&ES may be regulated by the lncRNA *Gm45349* and that *Hsd3b3*A3SS may be regulated by the lncRNA *Gm19619* (Fig. 7C–D). Furthermore, through RT−qPCR validation on liver tissues from different model mice, we examined

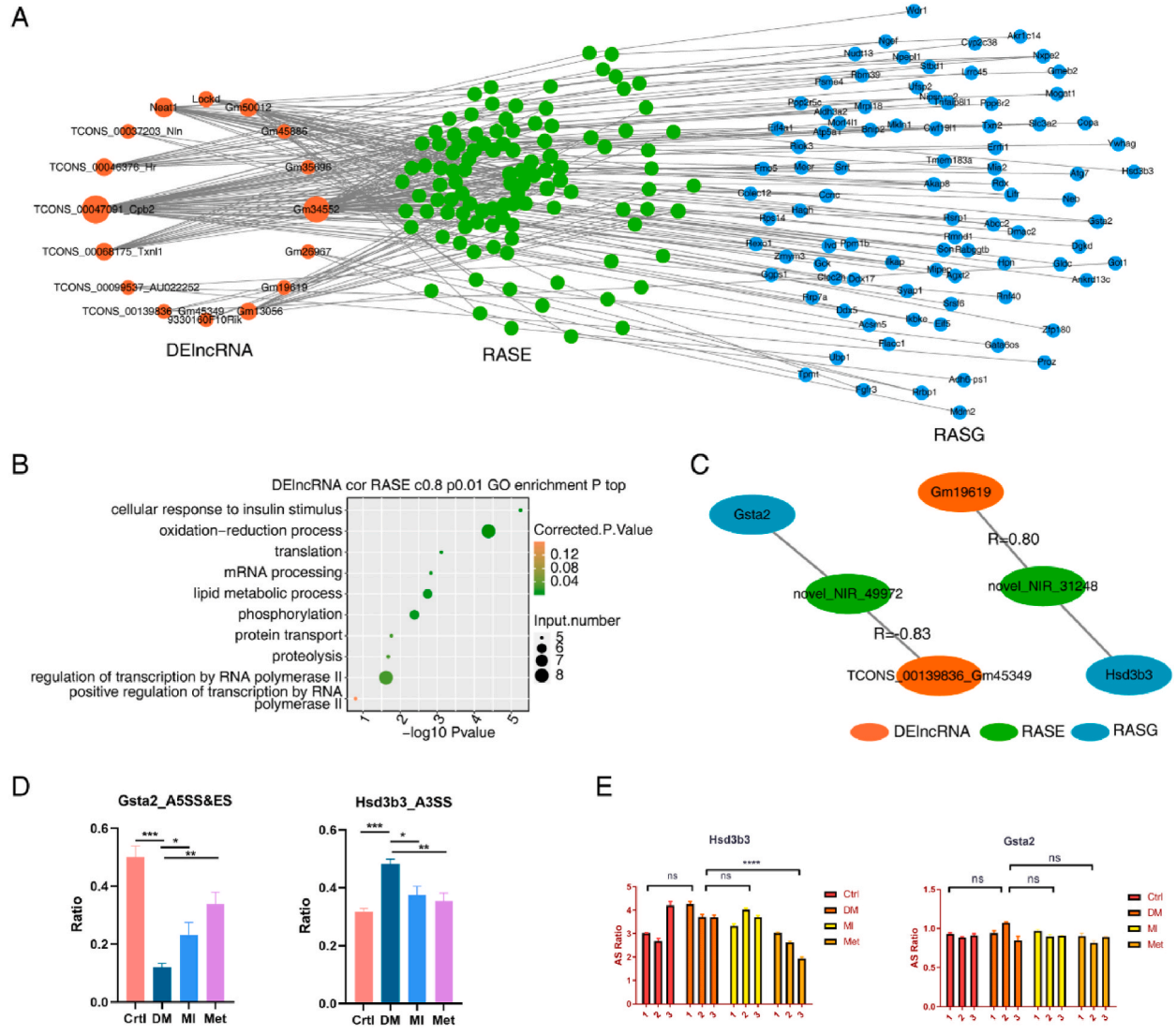

Fig. 7. Correlation analysis of lncRNAs and RASEs in liver tissues of diabetes mice after myo-inositol or metformin treatment. (A) Network plot showing the co-expression analysis of 17 DElncRNAs and alternative splicing genes (RASGs). The correlation coefficient is required to be greater than 0.8. (B) Bubble plot exhibiting the most enriched GO biological process results of the RASGs in Fig4A. (C) Network plot showing the target lncRNAs and co-expressed RASE, the correlation coefficient is indicated. (D) The alternative splicing events regulated by diabetes after myo-inositol or metformin treatment. The boxplot shows alternative splicing events of Gsta2 and Hsd3b3. (E) RT-qPCR detection of mouse gene ASEs between diabetes vs normal and myoinositol or metformin vs diabetes.

alternative splicing events for these two genes. We observed a significant increase in the ratio of alternative splicing events in the *Hsd3b3* gene in the Met group, which was consistent with our expectations (Fig. 7E).

3.8. Coexpression analysis and functional enrichment analysis of lncRNAs and RASEs in liver tissues of diabetic mice after myo-inositol treatment

The 16 lncRNAs (14 downregulated and 2 upregulated) that were specifically altered by MI treatment were coexpressed with the RASEs obtained in this study, and the results showed that these lncRNAs were coexpressed with 88 RASEs with a correlation coefficient >0.8 and P < 0.01 (Fig. 8A). GO functional enrichment analysis of the genes associated with these RASEs revealed enrichment in biological processes related to the response of cells to insulin stimulation, lipid metabolism, and diabetes (Fig. 8B).

The expression of 88 RASEs overlapped with that of 201 (113 downregulated and 88 upregulated) RASEs that were specifically altered by MI treatment, and 4 credible RASEs, namely, *Entpd5* A5SS, *Rrbp1* ES, *Nxpe2* ES, and thiopurine S-methyltransferase (*Tpmt*) A3SS, were identified based on significant differences in the ratios between the groups (Fig. 8D). The results of the coexpression

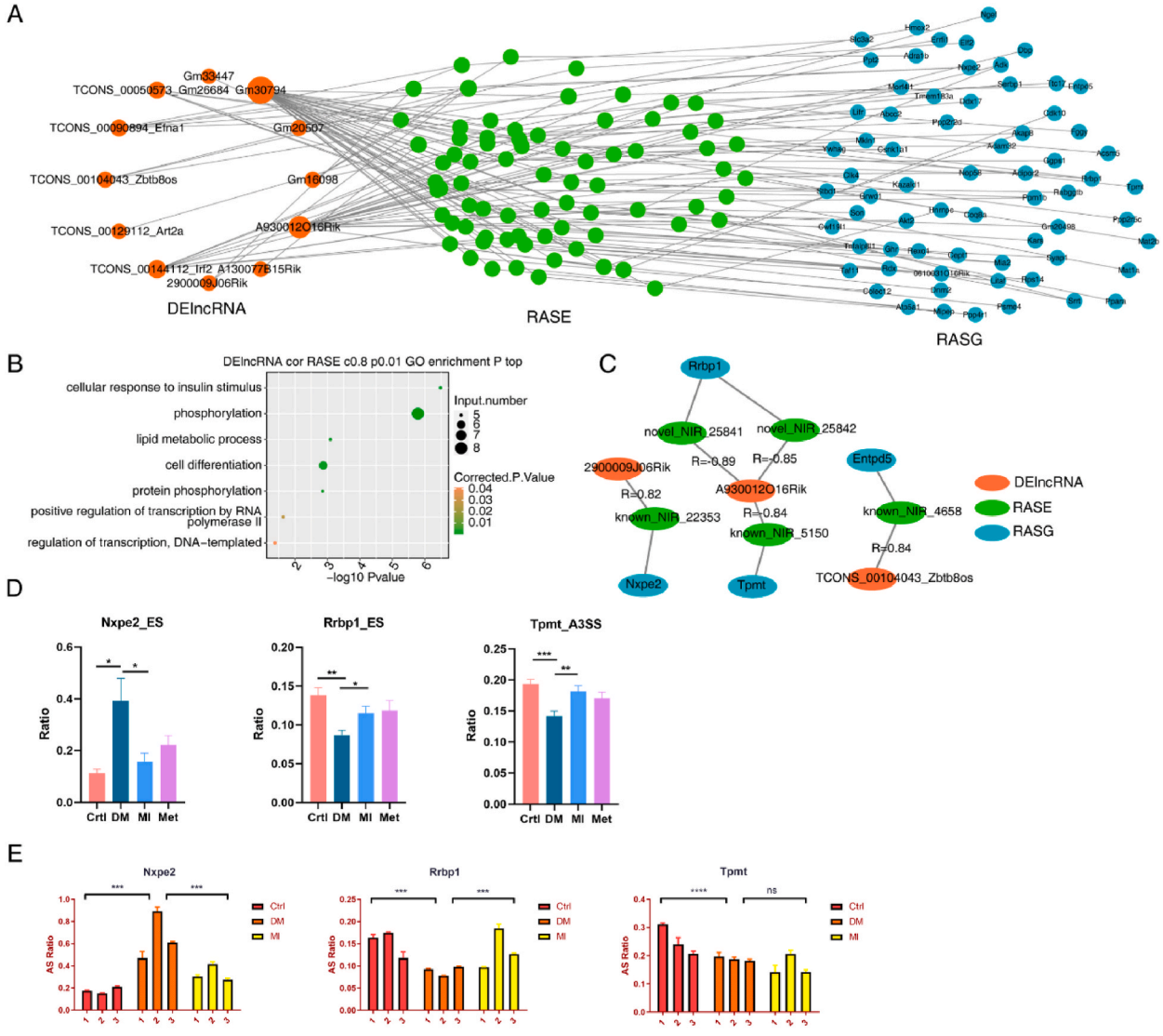

Fig. 8. Correlation analysis of lncRNAs and RASEs specific regulated by myo-inositol treatment. (A) Network plot showing the co-expression analysis of 16 DElncRNAs and alternative splicing genes (RASGs). The correlation coefficient is required to be greater than 0.8. (B) Bubble plot exhibiting the most enriched GO biological process results of the RASGs in Fig5A. (C) Network plot showing the target lncRNAs and co-expressed RASE, the correlation coefficient is indicated. (D) The alternative splicing events regulated by diabetes after myo-inositol treatment. The boxplot shows alternative splicing events of Nxpe2, Rrbp1, and Tpmt. (E) RT-PCR detection of ASEs for these three genes between diabetes vs normal and myoinositol vs diabetes.

network analysis showed that the lncRNAs *A930012016RIK, 2900009J06RIK,* and *TCONS_00104043_ZBTB8OS* may regulate *Rrbp1* ES and *Tpmt* A3SS, as well as *Nxpe2* ES and *Entpd5* A5SS (Fig. 8C). Furthermore, we also assessed the alternative splicing events for these three genes by RT−PCR. We found that the ratio of alternative splicing events in the *Tpmt* and *Rrbp1* genes increased in the DM group but decreased in the MI group. In contrast, for the *Nxpe2* gene, the opposite trend was observed. These findings were consistent with our predictions (Fig. 8E).

4. Discussion

The liver is widely recognized as the primary organ involved in glucose and lipid metabolism. In the context of hyperglycaemia, an imbalance in free fatty acid synthesis and metabolism can result in nonalcoholic fatty liver disease (NAFLD), which is characterized by excessive deposits of intrahepatic fat [19,20], as well as other disorders of lipid metabolism. The purpose of this study was to investigate the effects of MI on liver glucose and lipid metabolism in T2DM mice induced by a high-fat diet combined with streptozotocin. Our RNA-seq and bioinformatics analyses revealed that MI treatment significantly altered the levels of RASEs and lncRNAs in the T2DM mouse model. Moreover, through the coexpression analysis of lncRNAs and RASEs, we identified several key alternative splicing forms of lncRNAs that are relevant to liver glucose and lipid metabolism.

Through deep RNA-seq, we found that the levels of 105 RASEs in the livers of diabetic mice changed regardless of whether they were subjected to MI or met treatment. In addition, MI specifically altered 201 RASEs. Among the 105 RASEs affected by both MI and Met, 5 pivotal RASEs were identified. These RASE-related genes were *Homx2*, *Zfp467*, *Hnf4a*, *Ing1* and *Apoe*. Currently, many studies have focused mainly on proteins translated from these gene messages, but the alternative splicing of gene transcripts has rarely been investigated. Moreover, six key genes associated with RASEs, namely, *Entpd5, Mat1a, Eci2, Mlxipl, Klc1,* and *Rrbp1*, were identified among the 201 Rases whose expression changed only in response to MI. The alternative splicing events of these genes may play an important role in improving dysglycaemia and lipid metabolism disorders in diabetic livers through MI treatment.

In this study, significant differences in the expression of numerous lncRNAs were observed in the livers of diabetic mice treated with MI and Met. Compared to those in the normal diet group, 518 lncRNAs in the DM group had significantly altered expression, while 50 and 127 lncRNAs in the MI and Met treatment groups, respectively, had differentially expressed levels similar to those in the DM group. Furthermore, overlap analysis revealed that 17 lncRNAs were affected by both MI and Met. *Neat1* is a long noncoding RNA that is predominantly located in the nucleus and plays a crucial role in the formation of "paraspeckles" [21]. Studies have shown a significant upregulation of *Neat1* expression in the peripheral blood mononuclear cells of individuals with type 2 diabetes and newly diagnosed type 1 diabetes [22,23]. Following the knockdown of *Neat1* in hepatocellular carcinoma cells, the levels of intracellular free fatty acids and glycerol diester were shown to decrease; however, this effect was prevented by the overexpression of adipose triacylglyceride lipase (ATGL), suggesting that *Neat1* influences lipolysis in hepatoma cells through ATGL [24]. Furthermore, RNA sequencing revealed that *Neat1* expression was significantly increased in the livers of diabetic mice but significantly decreased after MI treatment, indicating that the effect of MI on *Neat1* expression may contribute to the mechanisms underlying improved liver fat metabolism and reduced inflammatory cell infiltration. Chen et al. revealed that the low expression of the lncRNA *Lockd* could aggravate liver fat deposition through the autophagy pathway [25]. Additionally, *Lockd* positively regulates the transcription of cyclin-dependent kinase inhibitor 1B (CDKN1B) through an enhancer-like *cis*-element [26], which has been reported to be involved in insulin secretion and glucose metabolism [27]. Our results showed that both MI and Met significantly decreased the expression of the lncRNA *Lockd* in the liver tissue of DM mice, suggesting that these two treatments might improve liver metabolic abnormalities through a *Lockd*-mediated mechanism.

Among the 16 lncRNAs specifically regulated by MI, the lncRNA *Gm16551* has been predicted to be related to lipid metabolism. One study showed that *Gm16551* negatively regulates lipogenesis by interacting with sterol regulatory element-binding protein-1c (SREBP-1c) [28]. In our analysis, *Gm16551* expression in the livers of diabetic mice distinctly decreased, but after MI treatment, it increased markedly, which is consistent with the above findings. Some researchers have extracted two datasets on differentially expressed genes between NAFLD models and normal control mouse liver tissues from the GEO database and conducted overlapping analysis. *Gm16551* was also among the commonly downregulated genes, which is consistent with our sequencing prediction results [29]. In addition, MI dramatically changed the expression of lncRNAs such as *Gm20507, Gm30794*, and *A930012O16RIK* in the liver. Some of these lncRNAs have not yet been annotated, and few studies have been conducted on them. The specific functions and mechanisms of these lncRNAs need to be further investigated.

This study investigated the coexpression and GO analyses of DElncRNAs and regulated alternative splicing genes (RASGs) in the liver tissues of diabetic mice after Met and MI treatment. GO enrichment analysis revealed that RASGs were enriched in biological processes such as cellular response to insulin stimulation, the oxidation−reduction process, translation, mRNA processing, and lipid metabolism. In the coexpression network analysis, we observed coexpression of genes, including *Gm45349/Gsta2* 5ASS&ES, *Gm19619/Hsd3b3* A3SS, A930012O16RIK/*Rrbp1* ES, A930012O16RI/*Tpmt* A3SS, 2900009J06RIK/NXPE2 ES, and TCONS_00104043_ZBTB8OS/*Entpd5* A5SS. *Rrbp1* is involved in the regulation of liver lipid homeostasis [30]. Furthermore, our qPCR study confirmed that the 3pMXE splicing mode of the *Rrbp1* gene increased following MI treatment. This observation suggests that the 3pMXE splicing mode of the *Rrbp1* gene could serve as a focal point for research on how MI contributes to the enhancement of glucose and lipid metabolism in the liver. *Entpd5* is involved in protein glycosylation and glycolysis [31]. Previous studies have shown that *Gsta2* is one of the core genes involved in the occurrence of diabetes through transcriptome analysis and PPI analysis [32]. The *Hsd3b3* gene phenotype is associated with changes in insulin sensitivity in patients with polycystic ovary syndrome [33]. Gene polymorphisms of *Tpmt* are associated with the hypoglycaemic effect of drugs [34]. LncRNAs may play an important role in the occurrence and development of diabetic liver steatosis and the improvement of diabetic liver disease by MI through the regulation of these coexpressed

RASEs.

In summary, this study provided an integrated characterization of diabetic hepatic transcriptomes with regard to lncRNAs and alternative splicing. Liver transcriptome analysis revealed that MI altered the AS of pre-mRNA and lncRNA expression in the livers of diabetic mice. The splicing of pre-mRNAs of genes involved in glycolipid metabolism was altered by MI, which may be a crucial mechanism for improving diabetic glycolipid metabolism disorder and hepatic steatosis. Moreover, lncRNAs may play an important role in regulating alternative splicing. This study provides a foundation for further exploration of the novel role and/or mechanism of MI.

Ethics declarations

This study was reviewed and approved by Experimental Animal Welfare Ethics Committee of Nanchang University, with the approval number: NCULAE-20221031042.

Funding

This work was supported by the National Natural Science Foundation of China (Grant No.82160162 and 81760150); Key project of Jiangxi Provincial Natural Science Foundation (Grant No.20202ACBL206008); Project of the Second Affiliated Hospital of Nanchang University (2022efyA04).

Informed consent statement

Informed consent was obtained from all subjects involved in the study.

Data availability statement

Data associated with our study has not been deposited into a publicly available repository. The authors are unable or have chosen not to specify which data has been used. The data presented in this study are available on request from the corresponding author.

CRediT authorship contribution statement

Jin'e Li: Writing – original draft, Investigation, Conceptualization. **Qiulan Huang:** Investigation, Data curation. **Qin Nie:** Investigation. **Yunfei Luo:** Resources, Methodology. **Haixia zeng:** Validation, Project administration. **Yuying Zhang:** Supervision. **Xiaoju He:** Supervision. **Jianping Liu:** Writing – review & editing, Conceptualization.

Declaration of competing interest

The authors declare that they have no known competing financial interests or personal relationships that could have appeared to influence the work reported in this paper.

Appendix A. Supplementary data

Supplementary data to this article can be found online at https://doi.org/10.1016/j.heliyon.2024.e32460.

References

[1] D.J. Magliano, E.J. Boyko, I.D.F.D.A.t.e.s. committee, IDF Diabetes Atlas. Idf Diabetes Atlas, vol. 2021, International Diabetes Federation © International Diabetes Federation, Brussels, 2021.
[2] A. Kotronen, A. Seppälä-Lindroos, R. Bergholm, H. Yki-Järvinen, Tissue specificity of insulin resistance in humans: fat in the liver rather than muscle is associated with features of the metabolic syndrome, Diabetologia 51 (1) (2008) 130–138.
[3] A. Seppälä-Lindroos, S. Vehkavaara, A.M. Häkkinen, T. Goto, J. Westerbacka, A. Sovijärvi, et al., Fat accumulation in the liver is associated with defects in insulin suppression of glucose production and serum free fatty acids independent of obesity in normal men, J. Clin. Endocrinol. Metab. 87 (7) (2002) 3023–3028.
[4] M.L. Croze, C.O. Soulage, Potential role and therapeutic interests of myo-inositol in metabolic diseases, Biochimie 95 (10) (2013) 1811–1827.
[5] M. Bizzarri, S. Dinicola, A. Cucina, Modulation of both insulin resistance and cancer growth by inositol, Curr Pharm Des 23 (34) (2017) 5200–5210.
[6] P.J. Antony, G.R. Gandhi, A. Stalin, K. Balakrishna, E. Toppo, K. Sivasankaran, et al., Myoinositol ameliorates high-fat diet and streptozotocin-induced diabetes in rats through promoting insulin receptor signaling, Biomed. Pharmacother. 88 (2017) 1098–1113.
[7] B. Pintaudi, G. Di Vieste, M. Bonomo, The effectiveness of myo-inositol and D-chiro inositol treatment in type 2 diabetes, Int J Endocrinol 2016 (2016) 9132052.
[8] L. Shi, X.T. Yu, H. Li, G.S. Wu, H.R. Luo, D-chiro-inositol increases antioxidant capacity and longevity of Caenorhabditis elegans via activating Nrf-2/SKN-1 and FOXO/DAF-16, Exp. Gerontol. 175 (2023) 112145.
[9] J. Juan-Mateu, O. Villate, D.L. Eizirik, Mechanisms in endocrinology: alternative splicing: the new frontier in diabetes research, Eur. J. Endocrinol. 174 (5) (2016) R225–R238.
[10] M. Song, L. Zou, L. Peng, S. Liu, B. Wu, Z. Yi, et al., LncRNA NONRATT021972 siRNA normalized the dysfunction of hepatic glucokinase through AKT signaling in T2DM rats, Endocr. Res. 42 (3) (2017) 180–190.

[11] A.R. Odom, A. Stahlberg, S.R. Wente, J.D. York, A role for nuclear inositol 1,4,5-trisphosphate kinase in transcriptional control, Science 287 (5460) (2000) 2026–2029.
[12] L. Jin, G. Li, D. Yu, W. Huang, C. Cheng, S. Liao, et al., Transcriptome analysis reveals the complexity of alternative splicing regulation in the fungus Verticillium dahliae, BMC Genom. 18 (1) (2017) 130.
[13] V.A. Cornelius, J.R. Fulton, A. Margariti, Alternative splicing: a key mediator of diabetic vasculopathy, Genes 12 (9) (2021).
[14] C. Pastori, C. Wahlestedt, Involvement of long noncoding RNAs in diseases affecting the central nervous system, RNA Biol. 9 (6) (2012) 860–870.
[15] Q. Pan, O. Shai, L.J. Lee, B.J. Frey, B.J. Blencowe, Deep surveying of alternative splicing complexity in the human transcriptome by high-throughput sequencing, Nat. Genet. 40 (12) (2008) 1413–1415.
[16] R.F. Luco, M. Allo, I.E. Schor, A.R. Kornblihtt, T. Misteli, Epigenetics in alternative pre-mRNA splicing, Cell 144 (1) (2011) 16–26.
[17] N. Romero-Barrios, M.F. Legascue, M. Benhamed, F. Ariel, M. Crespi, Splicing regulation by long noncoding RNAs, Nucleic Acids Res. 46 (5) (2018) 2169–2184.
[18] S. L'Abbate, G. Nicolini, F. Forini, S. Marchetti, N. Di Lascio, F. Faita, et al., Myo-inositol and d-chiro-inositol oral supplementation ameliorate cardiac dysfunction and remodeling in a mouse model of diet-induced obesity, Pharmacol. Res. 159 (2020) 105047.
[19] A.L. Birkenfeld, G.I. Shulman, Nonalcoholic fatty liver disease, hepatic insulin resistance, and type 2 diabetes, Hepatology 59 (2) (2014) 713–723.
[20] J. Mohamed, A.H. Nazratun Nafizah, A.H. Zariyantey, S.B. Budin, Mechanisms of Diabetes-Induced Liver Damage: the role of oxidative stress and inflammation, Sultan Qaboos Univ Med J 16 (2) (2016) e132–e141.
[21] S. Souquere, G. Beauclair, F. Harper, A. Fox, G. Pierron, Highly ordered spatial organization of the structural long noncoding NEAT1 RNAs within paraspeckle nuclear bodies, Mol. Biol. Cell 21 (22) (2010) 4020–4027.
[22] M. Alfaifi, M.M. Ali Beg, M.Y. Alshahrani, I. Ahmad, A.G. Alkhathami, P.C. Joshi, et al., Circulating long non-coding RNAs NKILA, NEAT1, MALAT1, and MIAT expression and their association in type 2 diabetes mellitus, BMJ Open Diabetes Res Care 9 (1) (2021).
[23] A.S. Santos, E. Cunha-Neto, N.V. Gonfinetti, F.B. Bertonha, P. Brochet, A. Bergon, et al., Prevalence of inflammatory pathways over immuno-tolerance in peripheral blood mononuclear cells of recent-onset type 1 diabetes, Front. Immunol. 12 (2021) 765264.
[24] X. Liu, Y. Liang, R. Song, G. Yang, J. Han, Y. Lan, et al., Long non-coding RNA NEAT1-modulated abnormal lipolysis via ATGL drives hepatocellular carcinoma proliferation, Mol. Cancer 17 (1) (2018) 90.
[25] R. Chen, H. Yang, Y. Song, H. Yu, M. Zhang, W. Rao, et al., Maternal obesity induces liver lipid accumulation of offspring through the lncRNA Lockd/mTOR autophagy pathway, Mol Genet Genomics 297 (5) (2022) 1277–1287.
[26] V.R. Paralkar, C.C. Taborda, P. Huang, Y. Yao, A.V. Kossenkov, R. Prasad, et al., Unlinking an lncRNA from its associated cis element, Mol Cell 62 (1) (2016) 104–110.
[27] T. Uchida, T. Nakamura, N. Hashimoto, T. Matsuda, K. Kotani, H. Sakaue, et al., Deletion of Cdkn1b ameliorates hyperglycemia by maintaining compensatory hyperinsulinemia in diabetic mice, Nat Med 11 (2) (2005) 175–182.
[28] L. Yang, P. Li, W. Yang, X. Ruan, K. Kiesewetter, J. Zhu, et al., Integrative transcriptome analyses of metabolic responses in mice define pivotal LncRNA metabolic regulators, Cell Metab 24 (4) (2016) 627–639.
[29] C. Hou, W. Feng, S. Wei, Y. Wang, X. Xu, J. Wei, et al., Bioinformatics analysis of key differentially expressed genes in nonalcoholic fatty liver disease mice models, Gene Expr. 19 (1) (2018) 25–35.
[30] M. Fang, Z. Shen, S. Huang, L. Zhao, S. Chen, T.W. Mak, et al., The ER UDPase ENTPD5 promotes protein N-glycosylation, the Warburg effect, and proliferation in the PTEN pathway, Cell 143 (5) (2010) 711–724.
[31] I. Anastasia, N. Ilacqua, A. Raimondi, P. Lemieux, R. Ghandehari-Alavijeh, G. Faure, et al., Mitochondria-rough-ER contacts in the liver regulate systemic lipid homeostasis, Cell Rep. 34 (11) (2021) 108873.
[32] Q. Ge, F. Feng, L. Liu, L. Chen, P. Lv, S. Ma, et al., RNA-Seq analysis of the pathogenesis of STZ-induced male diabetic mouse liver, J Diabetes Complications 34 (2) (2020) 107444.
[33] G. Carbunaru, P. Prasad, B. Scoccia, P. Shea, N. Hopwood, F. Ziai, et al., The hormonal phenotype of Nonclassic 3 beta-hydroxysteroid dehydrogenase (HSD3B) deficiency in hyperandrogenic females is associated with insulin-resistant polycystic ovary syndrome and is not a variant of inherited HSD3B2 deficiency, J. Clin. Endocrinol. Metab. 89 (2) (2004) 783–794.
[34] X. Li, F.M. Lian, D. Guo, L. Fan, J. Tang, J.B. Peng, et al., The rs1142345 in TPMT affects the therapeutic effect of traditional hypoglycemic herbs in prediabetes, Evid Based Complement Alternat Med 2013 (2013) 327629.